SHUTTLE ORBITER BOUNDARY LAYER TRANSITION

AT FLIGHT AND WIND TUNNEL CONDITIONS

Winston D. Goodrich and Stephen M. Derry
NASA Johnson Space Center
Houston, Texas

John J. Bertin
The University of Texas at Austin
Austin, Texas

ABSTRACT

Hypersonic boundary layer transition data obtained on the windward centerline of the Shuttle orbiter during entry for the first five flights are presented and analyzed. Because the orbiter surface is composed of a large number of thermal protection tiles, the transition data include the effects of distributed roughness arising from tile misalignment and gaps. These data are used as a benchmark for assessing and improving the accuracy of boundary layer transition predictions based on correlations of wind tunnel data taken on both aerodynamically rough and smooth orbiter surfaces. By comparing these two data bases, the relative importance of tunnel free-stream noise and surface roughness on orbiter boundary layer transition correlation parameters can be assessed. This assessment indicates that accurate predications of transition times can be made for the orbiter at hypersonic flight conditions by using roughness-dominated wind tunnel data. Specifically, times of transition onset and completion can be accurately predicted using a correlation based on critical and effective values of a roughness Reynolds number previously derived from wind tunnel data.

INTRODUCTION

During the design, development, and construction of the Space Shuttle orbiter, concerns regarding the sensitivity of the thermal protection system (TPS) design to changes in heat transfer rates and loads caused by boundary layer transition were paramount. These concerns were fueled by very preliminary studies[1] which showed that the weight of the TPS changed by approximately 25%, depending on which of several "universal" transition prediction methodologies were used. Because at this time only a limited aerothermodynamic data base existed for vehicles as complex as the orbiter, the design, development, and construction processes for the TPS commenced before more specific correlations could be developed. In particular, the TPS was sized using smooth surface transition predictions derived from orbiter wind tunnel data and correlated with the popular transition parameter Re_θ/M. To prevent premature roughness-induced transition, smoothness constraints were placed on the TPS based on the "effective" roughness concept developed by van Driest and Blumer[2]. However, as the TPS was being fabricated, it became apparent that the initial smoothness requirements (k = 0.017" to 0.04") could not be achieved without expensive and lengthy manufacturing and installation efforts. This prompted the development of a more refined aerothermodynamic data base with complementary flow field analyses[3,4] resulting in more refined orbiter heating and boundary layer transition prediction methodologies.[5,6,7] Because the orbiter windward surface is composed of a large number of TPS tiles, the transition criterion had to

include the effects of distributed roughness arising from tile misalignments and gaps. The individual tiles and gaps are visible in the photograph shown in Fig. 1.

Although the development of these methodologies could not always support the orbiter TPS design and construction schedule, the results were very useful in providing more quantitative estimates of aerothermodynamic uncertainties[8] necessary to support safety requirements for man-rated spacecraft operations. Furthermore, with regard to boundary layer transition, the analyses performed in Refs. 5, 6, and 7, which better defined the sensitivity of orbiter boundary layer transition to surface roughness caused by these TPS tile misalignments and gaps, allowed the stringent surface smoothness requirements initially imposed on the orbiter to be relaxed. In so doing, excessive concerns regarding TPS tile manufacturing and installation tolerances were also reduced, which contributed to an earlier rollout and flight schedule for the orbiter.

The transition methodology developed in Ref. 7, which was used extensively for making preflight assessments of the effects of surface roughness on orbiter boundary layer transition, is based on a relatively straightforward extrapolation of wind tunnel data correlations to flight conditions using local flow field parameters. This methodology requires precise geometric and dynamic flow simulation, which is a necessary condition for simulating both the magnitude and distribution of local flow field properties. Application to orbiter flight conditions was made on the premise that uncertainties in boundary layer transition data from hypersonic wind tunnels are always conservative; i.e., it is "well known" that boundary layer transition on a wind tunnel model occurs at lower Reynolds numbers than in flight because of disturbances or noise within the tunnel free stream. However, this premise is true only for aerodynamically smooth bodies, or bodies with roughness heights and/or other shock-layer-induced flow disturbances that do not dominate the transition process. Studies (Refs. 2, 9, and 10) aimed at defining the combined effects of roughness and free-stream disturbances for simple bodies with localized roughness elements have been conducted for the subsonic and supersonic flow regimes. Fewer studies have addressed the same issue for configurations as complicated as the orbiter while at hypersonic flow conditions and low values of T_w/T_0 and with the additional complexity of having multiple sources of flow disturbances, such as distributed roughness elements, wind tunnel free-stream noise, and disturbances from the curved bow shock entropy gradient.

With the completion of the Space Transportation System (STS) test flights, a substantial aerothermodynamic data base has been compiled which provides the opportunity to evaluate the orbiter boundary layer transition prediction methodology. To this end, the primary purpose of this paper is to provide additional information and insight into the requirements for developing a reliable transition methodology based primarily on wind tunnel data because, in most cases, only wind tunnel data exist on a given configuration at the time that critical design decisions need to be made for the project. In addition, this paper will present transition data from the first five flights of the orbiter in a form usable to the technical community, make comparisons of these data with previously published wind tunnel data, show comparisons of predicted transition times with flight data, and use the results of these comparisons to assess and improve the accuracy of the current[7] orbiter boundary layer transition prediction methodology. Emphasis will be placed on reviewing the wind tunnel data in l.,   of the STS flight data in order to establish a transition prediction methodology   the orbiter that will be less dependent on free-stream disturbances that exist   the wind tunnel. To accomplish this, the relative importance of tunnel free-stream noise and surface roughness on boundary layer transition distributions will be established from the data bases. In an effort to present the

754

data as completely as possible, several common transition parameters were used in making the comparisons ($Re\infty_{,L}$, Re_X, $Re\theta/M$, and Re_k). Care was also taken to assure that comparable ranges of flow conditions and vehicle attitudes were used. Because most of the transition parameters are defined using local flow conditions, results will be limited to the orbiter windward centerline where flow conditions can be accurately predicted based on correlations of the 3-D flow field results of Ref. 3.

ORBITER FLIGHT TEST (OFT) PROGRAM

The OFT program, consisting of the first four STS flights, was designed to provide information to certify the hardware for the orbiter subsystems and the methodologies used to design these subsystems. This was safely accomplished by planning these flights to provide relatively benign conditions for the orbiter at first, with each successive flight progressively stressing the orbiter subsystems closer to design levels. The fifth flight, although officially an operational flight, also provided data of a redundant nature that can also be used for certification purposes. Transition data from all five flights were utilized to fulfill the purposes of this paper.

Flight Instrumentation

For these developmental flights, an onboard instrumentation system, referred to as the development flight instrumentation (DFI), provided the data necessary for certification studies. Although quite extensive, only the locations of the surface thermocouples (thermocouples located within selected TPS tiles which were in contact with the TPS coating) required for this study will be described. Additional information concerning the DFI instruments and locations can be found in Ref. 11. Instrumentation used to define transition along the orbiter windward centerline is depicted in Fig. 2. Detailed locations of these instruments, along with orbiter "body point" numbers and instrument identification numbers, are listed in Table 1.

Because of various malfunctions with the DFI data recorder, entry data for STS-1 and STS-4 were obtained by telemetry for the portion of entry occurring after blackout. Approximately the first 1050 seconds of data were lost for these flights. Despite these problems, the complete transition location history was obtained on STS-4 and roughly half of it was obtained in STS-1. Data were obtained through the complete entries of STS-2, STS-3, and STS-5.

Surface Roughness

To estimate the effects of surface roughness on transition, information defining the magnitude and distribution of roughness over the orbiter is necessary. Referring again to Fig. 1, the qualitative features of roughness resulting from the TPS tile misalignments and gaps are readily visible. The majority of these tiles are 6" square with gaps ranging from 0.045" to 0.06". However, quantitative features of these roughnesses are difficult to obtain and as yet have not been determined. Nevertheless, an estimate of the roughness was made for the purposes of this paper. This estimate was based on two sources of data. First, tile misalignment heights were measured on vibro-acousic test panels used to simulate the response of orbiter structural panels and TPS tiles to vibration and acoustic loads experienced during launch. Tile misalignment heights were measured before and

after the tests. The measurements formed an approximate Gaussian distribution, with a mean value of approximately 0.03". Maximum values for these measurements were approximately 0.07".

Roughness estimates were also made using the distributions of allowable roughness used by the workers who installed the TPS tiles on the orbiter. As indicated in the Introduction, allowable roughness specifications were initially very stringent, but were eventually relaxed as more information was obtained on the effects of roughness on transition for the orbiter. Figure 3 illustrates the distribution of allowable roughness used to guide the initial installation of TPS tiles, in addition to the distribution used for the final phase of tile installation that was occurring at the time of orbiter rollout. The allowable roughness specifications used in the latter phase also included a specification on gap width $(k_a = (k^2 + (w - 0.045)^2)^{1/2})$. The effects of gaps were shown[12] to be somewhat less effective than misalignment height.

These are maximum allowable roughness distributions do not imply that all tiles were installed to these specifications. Because the tile installation procedures and materials used for the orbiter and the vibro-acoustic test models were nearly identical, similar Gaussian distributions of misalignment heights would be expected for each phase of the installation process. Therefore, the mean values can be estimated to be the average of the two ends of the distribution function for each installation phase (the average of zero and k_a, or $k_a/2$). Because the percentage of tiles installed during each phase was not readily available, and because of the nature of this estimate, the mean values of the final phase were used to provide an initial estimate of the surface roughness. This estimated roughness distribution is also shown in Fig. 3. This averaged roughness distribution and the vibro-acoustic model results were used as a guide in selecting roughness values to be used in calculating transition parameters that required roughness dimensions.

A significant, localized deviation to this roughness distribution occurred during the flight of STS-1. During this flight, ascent debris caused a large gouge (approximately 8" × 2" × 1" deep) in the TPS surface on the right forward landing gear door. This location is just off the centerline near x = 0.05L. The effect of this damage on the times of transition will be shown in a subsequent section.

Orbiter Test Conditions

The free-stream entry conditions for the OFT program are depicted in Fig. 4 by the dimensionless flow parameters $Re_{\infty, L}$ and M_∞. The range of these parameters used for the wind tunnel test program is also shown for reference. Identification of transition onset and completion is also indicated for each trajectory. Note that the onset value for STS-1 is not shown because of the DFI recorder malfunction. Also note that the location of transition onset is defined to be at the 99% length station (i.e., x = 0.99L). The location of transition completion was arbitrarily defined to be at x = 0.1L. This location was chosen because it essentially covered the complete orbiter centerline, and also because transition further forward occurred well past hypersonic flow conditions and was well outside the range of the wind tunnel data base. This occurred possibly because of the very favorable pressure gradient that is present along the forward 15% of the orbiter centerline. Predictions of the pressure distributions along the centerline are presented in Refs. 3 and 4. This result suggests that the orbiter roughness in this region is not as effective a boundary layer trip as the same roughness located further downstream.

This observation is basically consistent with the results presented by Morrisette[13], who showed that roughness in this region had to be two to seven times as large as roughness in low-pressure-gradient regions to be as effective at tripping the boundary layer.

The important point shown in Fig. 4 is that transition occurs over most of the centerline for a narrow range of relatively low free-stream Mach numbers. That is, transition starts near Mach 10, and is essentially complete near Mach 7. These conditions occur well past peak heating, and therefore contribute very little to the heat load experienced by the orbiter during entry. Also note that in terms of these parameters, the wind tunnel conditions provided a reasonable test environment.

To help relate these parameters to entry time, histories of free-stream Reynolds numbers are shown in Fig. 5 for all five flights. The times and values of $Re_{\infty,L}$ for transition onset and completion are also depicted, along with the range of $Re_{\infty,L}$ used in the wind tunnel test program. Because of planned trajectory differences, the times of transition onset and completion are observed to occur earlier with each successive OFT flight, except for STS-1, which has the earliest transition onset. This occurred because the TPS roughness on STS-1 was much greater than the other flights due to the previously discussed ascent debris damage. Note also that the values of $Re_{\infty,L}$ at transition onset and completion are approximately the same for each of the flights, with the exception of transition onset for STS-1. For operational purposes, this may be an adequate parameter for predicting transition. if the trajectories and roughness remain about the same.

Additional information regarding the entry trajectories is shown in Fig. 6, where histories of orbiter angle of attack are depicted along with the times of transition onset and completion. Note that, for all cases, the angles of attack for transition onset and completion are approximately 40° and 25°, respectively. For this angle-of-attack range, the wind tunnel data base indicated very little effect of angle of attack alone on transition.

The times used in the previous two figures were measured from entry interface, which is assumed to occur at approximately 4×10^5 feet altitude. For reference purposes, the Greenwich mean time (GMT) is listed in Table II along with the altitude, velocity, and angle of attack for each OFT mission. This will be useful when comparing these results to other interpretations of the flight data base.

DISCUSSION OF RESULTS

Temperature histories of the TPS surface, obtained from DFI surface thermocouples, were used to establish the times of boundary layer transition along the orbiter centerline. Locations of the instruments are shown in Fig. 2. Transition at a given instrument occurred when the temperature history deviated or jumped significantly from an otherwise smooth behavior. Figure 7 depicts typical surface temperature histories for instruments located along the centerline at $x = 0.1L$, $x = 0.5L$, and $x = 0.9L$ for STS-3. Transition times are indicated by the arrows. Examination of all the temperature histories in this manner was used to establish transition for all flights and instruments. Times of transition, along with all free-stream conditions necessary to calculate transition parameters, are listed in Table III for these flights and DFI instrument locations. Comparison of transition parameters obtained from these data will be made with wind tunnel test results in the next section.

Comparisons of Flight and Wind Tunnel Data

By comparing transition data from flight and hypersonic wind tunnels at comparable simulation conditions—and recognizing that the major difference in simulation parameters at these conditions was the level of free-stream noise—differences in transition results can be attributed to the presence of this free-stream noise. The objective of these comparisons will be to identify regions on the orbiter where these differences are at a minimum and use these results to improve the prediction methodology for the orbiter and to provide insight into the use of wind tunnel data for making similar predictions on other vehicles.

Free-Stream Conditions. The variations of the locations of transition with $Re_{\infty,L}$, calculated at the time of transition for these locations, are illustrated in Fig. 8. Also shown are the same parameters taken from the wind tunnel data base which used smooth and rough models. The first thing to note from this comparison is that the transition locations aft of $x = 0.15L$ appear to be much more sensitive to $Re_{\infty,L}$ for the flight data than the wind tunnel. In fact, at flight, transition moves forward to $x = 0.15L$ at approximately a constant Reynolds number. However, the Reynolds number at which this occurs varies somewhat from flight to flight. The behavior of the STS-1 data is an anomaly because of the additional surface roughness that occurred on this flight. However, these data do tend to follow the Reynolds number dependence of the wind tunnel data, possibly because of the overlapping effects of noise and roughness in the wind tunnel data. Also, because the very large localized roughness on STS-1 was off centerline, which may have caused early nonsymmetrical transition about the centerline, agreement with any correlation based on symmetrical data alone would be fortuitous. Insufficient data exist off centerline to verify this hypothesis. Another point concerning these data is that the wind tunnel and flight data are in relatively good agreement in the region between x/L of 0.1 to approximately 0.4. This suggests that the effects of free-stream noise may not be a significant factor in causing transition in this region because of other disturbances coming from surface roughness and the shock layer entropy gradient within the curved bow shock. Similar agreement will be shown for the transition parameters based on local flow conditions in the next section.

Local Flow Conditions. Predictions of local flow field and boundary layer properties have been made for most of the DFI locations along the orbiter centerli   for the STS missions. These predictions were based on correlations of numerical flowfield solutions made for the orbiter windward surface for the design trajectory using the methods developed in Ref. 3. Parameters relevant to correlating transition data have been predicted for these instrument stations at times of transition for each trajectory. These predictions are listed in Table IV.

Selected flow parameters (M, Re_x, Re_θ/M, and Re_k) from Table IV are graphically illustrated in Fig. 9, along with these same parameters obtained from the wind tunnel test program. Figure 9(a) shows distributions of the local Mach number at the times of transition for each centerline station. With rare exception, transition values of local Mach number, M_{tr}, obtained at 30° and 40° angle of attack at wind tunnel conditions embrace the values of M_{tr} predicted at flight conditions. Basically, these results show that the wind tunnel conditions provided an excellent simulation of local Mach numbers for the flight conditions associated with transition. In addition, the values of M_{tr} at transition are relatively low (i.e., $M_{tr} \leq 2.5$).

In Fig. 9(b), distributions of local Reynolds numbers obtained from the flight and wind tunnel transition results are presented. As expected, transition values of the local Reynolds number, $Re_{x,tr}$, at flight conditions are almost always higher

758

than values from the wind tunnel at comparable centerline locations. Actually, there is as much variation in the flight data as the wind tunnel data, which suggests that this parameter does not correlate the data very well. This is particularly true when both wind tunnel and flight data are considered. However, these distributions do reveal that some sources of flow disturbances may be present for the forward 40% of the orbiter, because both sets of data show a significant reduction in values of $Re_{x,tr}$ in this region. At flight conditions, these disturbances could come from a combination of shock layer gradients and surface roughness. In the wind tunnel, free-stream noise can be added to these disturbances. However, other factors may also be contributing this behavior and general lack of correlation using $Re_{x,tr}$. For example, $Re_{x,tr}$ alone does not correlate the effects of the boundary layer gradients or of surface roughness or temperature conditions, but only the effects of edge conditions.

In attempts to account for these differences and other flow parameters, investigators have developed a number of correlation parameters using various combinations of edge and boundary layer factors. Because it accounts for boundary layer properties as well as edge compressibility effects, Re_θ/M has evolved as one of the more popular forms of transition-correlating parameters and was selected here to represent this class of correlation parameter. Distributions of transition values of this parameter, $(Re_\theta/M)_{tr}$, for both wind tunnel and flight conditions are presented in Fig. 9(c). Again, possibly because of a combination of shock layer and surface roughness flow disturbances, significant reductions in the values of this parameter occur for the forward 40% of the orbiter at flight conditions. However, by using $(Re_\theta/M)_{tr}$ as a correlation parameter, the wind tunnel and flight data correlations are in better agreement in this region, but remain significantly different in the downstream region.

Thus far, the correlation parameters considered have not included the very important effects of surface roughness or of temperature. Braslow[14] and others have shown that the roughness Reynolds number, Re_k—a Reynolds number based on roughness height and boundary layer conditions at the top of the roughness--successfully correlates transition data over a range of local Mach numbers from approximately 0 to 4. In defining Re_k, values of surface roughness and temperature have to be known. For a given roughness, transition was shown[5,6,7] to be very sensitive to variations in surface temperature in the wind tunnel test program. This occurred because by cooling of the boundary layer, the density of the flow near the surface and at the top of the roughness would increase accordingly. Values of Re_k increased in proportion to the density. The effects of the changes in viscosity and velocity were less significant.

In the section covering surface roughness, the average roughness distribution was estimated to range from 0.03" to 0.1". To cover this range, transition values of the roughness Reynolds number, $Re_{k,tr}$, were calculated using three values of roughness: 0.03", 0.06", and 0.1". Values of $Re_{k,tr}$ for all three values of k, calculated using the surface temperature at flight, are listed in Table IV for all the flight transition times. Values of $Re_{k,tr}$ at wind tunnel conditions were calculated in Ref. 7 using the surface roughness and temperature conditions of the wind tunnel models. Figure 9(d) presents distributions of $Re_{k,tr}$ (using an average value of k = 0.06") from the flight and wind tunnel data bases. As before, large differences in the flight and wind tunnel data bases exist downstream of the 40% station, probably because of wind tunnel noise. However, agreement between these two data bases has improved in the upstream region using the correlation parameter $Re_{k,tr}$, which accounts for not only edge and boundary layer conditions but also accounts for surface roughness and temperature conditions. This suggests that the

effects of the surface conditions are dominant in the upstream region, while further downstream, the effects of tunnel noise dominate the transition process in wind tunnel tests. This further suggests that if transition distributions obtained from wind tunnel data were extrapolated to flight conditions, transition predictions would be conservative in the downstream region and reasonably reliable in the upstream region. This thought will be discussed in the next section, which compares predicted transition times with flight data for the orbiter centerline.

Transition Predictions

Using wind tunnel data alone, several transition prediction methodologies were developed in Refs. 5, 6, and 7. These methods all had one thing in common: the transition parameter (e.g., x_{tr}/L, $Re_{x,tr}$, $(Re_\theta/M)_{tr}$) used for making predictions of roughness-induced transition was correlated in terms of a departure from the same parameter correlated using smooth body data alone.[*] This departure was functionally related to a roughness parameter (e.g., δ^*/k or Re_k) using the wind tunnel data. For more details on these parameters and correlations, see Ref. 7.

The correlation judged best suited for making preflight predictions was based on a departure of Re_θ/M from the smooth-body transition values as a function of $Re_{k,x=0.1L}$. This was selected because the smooth body prediction methodology was already based on Re_θ/M (see Fig. 9(c)). This correlation, reproduced from Ref. 7, is shown in Fig. 10. The normalized or relative transition parameter ξ is the ratio of Re_θ/M at roughness-induced transition conditions to Re_θ/M at smooth surface conditions (i.e., $\xi = (Re_\theta/M)_{tr,R}/(Re_\theta/M)_{tr,S}$). The reference roughness Reynolds number $Re_{k,x=0.1L}$ is calculated at the 10% centerline station for the conditions of transition. Several factors were involved in selecting x = 0.1L as the reference location for calculating the transition parameter accounting for the effects of surface roughness and temperature. Initially, the orbiter was expected to have relatively uniform surface roughness, which suggested that any point might be adequate. Furthermore, at the time the correlation was developed, it was relatively difficult to calculate Re_k over the complete vehicle, but Re_k could be calculated relatively easily and accurately at x = 0.1L. However, the most important factor was the observation that when surface roughness and temperature effects did cause transition to move forward, transition would move to this general area. In addition, this location was at the end of the favorable pressure gradient region coming from the nose. Therefore, this location, which had the largest values of Re_k for low-pressure-gradient areas, would better reflect the effects of surface roughness on transition for the rest of the vehicle, which also had very low pressure gradients.

Also noted on Fig. 10 are the values of $Re_{k,x=0.1L}$ which cause transition to move forward at various rates on the orbiter. Surface roughness and cooling had no measurable effects on transition location for values of $Re_{k,x=0.1L}$ less than 30. This is defined as the incipient value of $Re_{k,x=0.1L}$ because it is the value that causes ξ to decrease just below unity. The effect of roughness and cooling on transition is minimal until $Re_{k,x=0.1L}$ reaches a value of 110, which is called the critical value. Above the critical value, the relative transition parameter decreases rapidly (transition moves rapidly upstream toward the nose) until $Re_{k,x=0.1L}$ reaches a value of 180. This is the minimum value of $Re_{k,x=0.1L}$ which will move transition the furthest forward for the test conditions. Therefore, 180 is defined as the effective value of $Re_{k,x=0.1L}$, because the roughness elements are now serving as effective tripping devices.

Preflight Predictions. The correlation shown in Fig. 10 served as the basic part of the preflight transition prediction methodology. The smooth surface transition correlation based on Re_θ/M, which is shown in Fig. 9(c), completes the methodology. To predict the locations of transition at flight, a history of the values of $Re_{k,x=0.1L}$ must be known for the trajectories. Such a history is shown in Fig. 11 for the STS trajectories. A nominal roughness value of 0.06" was used in calculating $Re_{k,x=0.1L}$. This value of k seemed to be a reasonable estimate based on all the considerations given in the roughness section. The effects of selecting different roughness sizes on the predictions of transition were investigated in Ref. 7 for the design trajectory.

To predict the location of transition for a given trajectory at a particular time, use Fig. 11 to determine the value of $Re_{k,x=0.1L}$ at this time. With this value, enter Fig. 10, and obtain a value of the relative transition parameter ζ. Knowing the smooth surface distribution of $(Re_\theta/M)_{tr,s}$ (as given by the correlation in Fig. 9(c)) and the value of ζ, the new value of $(Re_\theta/M)_{tr,R}$ that accounts for the effects of roughness on transition at this time can be calculated. With this value and a calculated distribution of Re_θ/M for this particular time, the roughness-induced transition location can be determined for this time. Histories of Re_θ/M have to be calculated for each trajectory. These calculations have been made for the five STS trajectories, and the resulting predictions of transition times are presented in Fig. 12 for the DFI locations given in Table IV. Predictions were not made for all the stations because local flow models were not available for the missing stations. The predicted times of transition follow the trends of the transition parameters shown in Figs. 8 and 9 in that the transition predictions based on wind tunnel data alone were very conservative downstream of the 30% to 40% stations. The exception observed for STS-1 in Fig. 12(a) occurs because of the previously mentioned TPS damage, resulting in a relatively large localized roughness just off centerline near the nose region. Predicted transition times forward of the 30% to 40% stations are in very good agreement with the data. These results are consistent with the previous discussion concerning roughness and the effects of free-stream disturbances on the tunnel data and resulting correlations. In addition, note that the predictions for x = 0.025L are very approximate because the prediction correlation did not include wind tunnel transition data from this very high pressure gradient region.

Postflight Comments. There are several ways that the prediction methodology can be improved. The first step would be to remove the smooth-surface data from the correlation parameter, because of its sensitivity to free-stream noise. However, as previously noted, even a large part of the rough-surface wind tunnel data in the downstream region seems to be sensitive to tunnel noise. To avoid this, one could simply correlate the flight data and possibly use the wind tunnel data to supplement the correlation. For example, for future operational flights, local values of Re_k that cause transition could be predicted by using the averages of the four previous flights. This methodology would be particularly useful if predictions of the effects of significant changes in roughness distributions are required. Also, by using this approach, the equivalent roughness size for STS-i could be estimated by trial and error. This may be a good thing to do to support operational requirements. However, the primary objective of this paper is "to provide additional information and insight into the requirements for developing a reliable transition methodology based primarily on wind tunnel data . . .".

The very good agreement between the predicted and measured transition times in the 10% to 20% centerline region suggests that the wind tunnel simulations and correlation of transition in this region must have been very good. This must have

occurred because surface roughness and shock layer disturbances dominated the transition process in this region at both wind tunnel and flight conditions. This was possible because of the relatively thin boundary layer and highly curved bow shock near the forward part of the orbiter. This is consistent with the discussion of Fig. 9(d). The fact that transition moves rapidly to the location of the effective roughness Reynolds number region, also in this region, is consistent with the findings of Ref. 7 shown in Fig. 10. One could conclude from this that transition times in this region could be predicted with the effective roughness Reynolds number obtained from the wind tunnel data.

This prediction of effective transition can be simply accomplished by entering Fig. 11 with the effective value of $Re_{k,x=0.1L}$ (i.e., 180) and extracting the times of effective transition in the 10% to 20% region for each trajectory. The results of this operation are shown in Fig. 12. The agreement with flight data is very good.

The fact that the flight transition moved forward so rapidly also suggests that the transition process occurs similarly to the process observed in the wind tunnel when the roughness Reynolds numbers were increasing from critical to effective values. The only difference between these tests was that for the wind tunnel tests the locations of transition were already on the orbiter when $Re_{k,x=0.1L}$ was critical, whereas for the flight tests transition was not yet on the orbiter. This occurred because tunnel noise and roughness both affect transition in the critical transition process, thus causing transition to be further forward at this time in the tunnel. Therefore, it could be possible to predict transition onset for the orbiter by using the critical value of $Re_{k,x=0.1L}$ (i.e., 110) just as was done using the effective value. These results are also indicated in Fig. 12. The agreement with transition onset is excellent for all flights except STS-1, which is as expected because of the differences in the surface roughness.

No attempt has been made to establish a prediction of the distribution of transition times between the critical and effective points. However, considering how quickly transition moves forward and the general uncertainties in the methodology, connecting the two points with a straight line should provide adequate predictions for design purposes.

CONCLUDING REMARKS

Surface temperature measurements from the windward centerline of the Shuttle orbiter have been used to define the locations of boundary layer transition during entry for the first five orbiter flights. Because the orbiter windward surface is composed of a large number of thermal protection tiles, the transition data include the effects of distributed roughness arising from tile misalignment and gaps. These data are used as a benchmark for assessing data from previous wind tunnel tests and for improving the accuracy of boundary layer transition predictions based on correlations of wind tunnel data taken on both aerodynamically rough and smooth orbiter models. Specifically, by comparing the data from these two environments, the relative importance of tunnel free-stream noise and of surface roughness on orbiter boundary layer transition predictions can be estimated. Based on these data, the following conclusions are made.

1) Free-stream disturbances dominate transition in the wind tunnel downstream of $x \cong 0.4L$. This conclusion is based on the observation that at early flight

762

times, transition locations based on wind tunnel data are significantly further upstream than those actually measured during flight. This occurs because the Reynolds number is relatively low, the boundary layer is relatively thick so that the tile-related roughness is submerged, and the wall temperature ratio, T_w/T_0, is low, which is usually considered as stabilizing. Because the wind tunnel simulation of local transition parameters was generally very good, "tunnel noise" is apparently a dominant factor in the transition process in the wind tunnel downstream of the 40% station. Since there are no corresponding background disturbances in the flight environment, transition occurs later in flight than one would predict using wind-tunnel-based correlations that use data from this noise-dominated region.

2) Surface roughness and, perhaps, shock layer disturbances dominate transition at both flight and wind tunnel conditions upstream of $x \cong 0.4L$. This is based on the fact that, at later flight times, the transition locations are in relatively good agreement with the predictions based on wind tunnel data. At these times, the Reynolds numbers are relatively high so that the boundary layer is relatively thin and, therefore, the tile-related roughness produces significant perturbations to the flow. Furthermore, the surface temperature has increased and T_0 has decreased, so that surface cooling is no longer as stabilizing as it was. Thus, the transition process is probably dominated by surface-roughness-induced perturbations and entropy gradient disturbances associated with the curved bow shock wave. Because the misaligned tiles are now serving as effective boundary layer trips, tunnel noise does not significantly influence the transition locations. Therefore, the measured locations of transition at flight are in relatively good agreement with wind-tunnel-based predictions.

3) Times of transition onset and completion at hypersonic flight conditions correspond to times when the reference roughness Reynolds number, $Re_{k,x=0.1L}$, reaches, respectively, its critical and effective values. These values, which are 110 and 180, respectively, were established from previous wind tunnel data analyses. This relationship can be used as a relatively simple improvement to the current transition prediction methodology. This is possible because these transition values are surface roughness dominated and, therefore, are relatively insensitive to the effects of wind tunnel noise.

SYMBOLS

k	height of the misaligned tiles
L	orbiter axial length, 107.75 ft
M	Mach number
Re_k	Reynolds number based on conditions at the top of the misaligned tile
Re_θ	Reynolds number based on local flow properties and the momentum thickness
$Re_{\infty,L}$	Reynolds number based on free-stream flow properties and the orbiter length
T	temperature

w	width of tile gaps
x	axial coordinate
α	angle of attack
σ^*	displacement thickness
θ	momentum thickness
ζ	relative transition location defined in Fig. 10

Subscripts:

o	evaluated at the stagnation conditions
tr	evaluated at the transition location
w	evaluated at the wall
∞	evaluated at the free-stream conditions

REFERENCES

1. Ried, R. C., Jr., Goodrich, W. D., Strouhai, G., and Curry, D. M., "The Importance of Boundary-Layer Transition to the Space Shuttle Design," Proceedings of the Boundary-Layer Transition Workshop held Nov. 3-5, 1971. Aerospace Report No. TOR-0172 (S2816-16) -5, Dec. 20, 1971.

2. van Driest, E. R., and Blumer, C. B., "Boundary-Layer Transition at Supersonic Speeds - Three-Dimensional Roughness Effects (Spheres)," Journal of the Aerospace Sciences, Aug. 1962, Vol. 29, No. 8, pp. 909-926.

3. Goodrich, W. D., Li, C. P., Houston, C. K., Chiu, P., and Olmedo, L., "Numerical Computations of Orbiter Flow Fields and Laminar Heating Rates", Journal of Spacecraft Rockets, May 1977, Vol. 14, No. 5, pp. 257-264.

4. Rakich, J. V. and Lanfranco, M. J., "Numerical Computation of Space Shuttle Laminar Heating and Surface Streamlines," Journal of Spacecraft and Rockets, May 1977, Vol. 14, No. 5, pp. 265-272.

5. Bertin, J. J., Idar, E. S., III, and Galanski, S. R., "Effect of Surface Cooling and Roughness on the Heating (Including Transition) to the Windward Plane-of-Symmetry of the Shuttle Orbiter", Aerospace Engineering Report 77002, Apr. 1977, The University of Texas at Austin.

6. Bertin, J. J., Idar, E. S., III, and Goodrich, W. D., "Effect of Surface Cooling and Roughness on Transition for the Shuttle Orbiter", Journal of Spacecraft and Rockets, March-April 1978, Vol. 15, No. 2., pp. 113-119.

7. Bertin, J. J., Hayden, T. E., and Goodrich, W. D., "Shuttle Boundary-Layer Transition Due to Distributed Roughness and Surface Cooling", Journal of Spacecraft and Rockets, Sept.-Oct. 1982, Vol. 19, No. 5, pp. 389-396.

8. Goodrich, W. D., Derry, S. M., and Maraia, R. J., "Effects of Aerodynamic Heating and TPS Thermal Performance Uncertainties on the Shuttle Orbiter," in Entry Heating and Thermal Protection, Vol. 69 of Progress in Astronautics and Aeronautics, Walter B. Olstad, ed. (1980) pp. 247-268.

9. Dryden, H. L., "Review of Published Data on the Effect of Roughness on Transition from Laminar to Turbulent Flow", Journal of the Aeronautical Sciences, July 1953, Vol. 20, No. 7, pp. 477-482.

10. Pate, S. R., "Induced Boundary-Layer Transition at Supersonic Speeds: Combined Effects of Roughness and Free-Stream Disturbances," May 1970, AIAA Paper 70-586.

11. Smith, J. A., "STS-3 Structural and Aerodynamic Pressure and Aerothermodynamic and Thermal Protection System Measurement Locations," Thermal Technology Branch ES3-82-1, NASA Johnson Space Center JSC 17889, Houston, TX, January 15, 1982.

12. Bertin, J. J. and Keisner, A., "Effects of Step and/or Gap Tile Misalignment on Shuttle Transition," Aerospace Engineering Report 78003, The University of Texas at Austin, June 1978.

13. Morrisette, E. L., "Roughness Induced Transition Criteria for Space Shuttle-Type Vehicles," Journal of Spacecraft and Rockets, February 1976, Vol. 13, No. 2, pp. 118-120.

14. Braslow, A. L., "A Review of Factors Affecting Boundary-Layer Transition", NASA TND-3384, Apr. 1966.

TABLE I.- IDENTIFICATION AND LOCATION OF FLIGHT
THERMOCOUPLES USED FOR SPECIFYING THE TIMES
OF BOUNDARY LAYER TRANSITION

Instrument identification number	Body point number	$\frac{x}{L}$	X,[a] in.	Y, in.
V09T9341	1020	0.0257	268.0	+1.2
V07T9452	1100	0.099	361.7	-4.9
V07T9462	1140	0.141	416.5	0.0
V07T9463	1160	0.164	446.2	-3.9
V07T9464	1200	0.196	486.5	-6.6
V09T9381	1250	0.257	565.0	-4.2
V09T9421	1300	0.288	604.7	-8.4
V07T9468	1300	0.299	618.9	0.0
V07T9471	1400	0.404	754.7	0.0
V09T9521	1500	0.501	878.9	-12.8
V07T9478	1600	0.598	1003.8	0.0
V07T9481	1700	0.695	1128.0	0.0
V07T9487	1800	0.801	1265.0	0.0
V07T9489	1900	0.900	1391.5	0.0
V09T9751	1950	0.952	1458.2	0.0
V07T9492	1990	0.993	1511.1	+1.3

[a]$X = x + 235.$

TABLE II.- MISSION TIMES USED TO DEFINE ENTRY
INTERFACE FOR EACH FLIGHT, ALONG WITH
SELECTED TRAJECTORY PARAMETERS

Mission number	Alt, ft	$\dot{V}_\infty$ ft/sec	α, deg	Mission time (GMT), sec
STS-1	399840	24555.8	41.22	9049750
STS-2	400141	24516.9	41.09	27550239
STS-3	400102	24451.5	40.97	7745683
STS-4	400049	24439.6	40.97	16040426.6
STS-5	400200	24398.0	40.83	27698594.9

TABLE III.- FREE-STREAM CONDITIONS AT TIMES OF BOUNDARY LAYER TRANSITION ALONG THE ORBITER WINDWARD PITCH PLANE

$\frac{x_{tr}}{L}$[a]	Time, sec	Alt, k-ft	V_∞, ft/sec	α, deg	T_∞, °R	p_∞, $\frac{lbf}{ft^2}$	$\rho_\infty \times 10^5$, $\frac{slugs}{ft^3}$	M_∞	$Re_{\infty,L}$ × 10^{-6}
					STS-1				
0.025	1716	33.8	722	7.8	394	548.5	81.16	0.74	211.
0.1	1357	121.1	5402	23.6	440	9.646	1.279	5.26	22.72
0.14	1320	131.3	6239	26.4	447	6.242	0.81	6.02	19.
0.16	1272	144.3	7377	30.5	463	3.683	0.4634	6.99	10.78
0.20	1272	144.3	7377	30.5	463	3.683	0.4634	6.99	10.78
0.25	1231	154.9	8469	34.5	480	2.448	0.2974	7.89	7.72
0.3	1220	156.4	8783	33.7	480	2.306	0.2800	8.17	7.53
0.4	1159	171.5	11279	38.6	464	1.278	0.1605	10.48	5.69
0.5	1136	172.2	11374	38.7	464	1.249	0.1568	10.77	5.41
0.6	<1052	184.7	14179	39.5	455	0.7535	0.0964	13.56	4.57
0.7									
0.8	No data prior to 1052 sec.								
0.9									
0.99									
					STS-2				
0.025	1710	41.	837	5.3	380	397.2	60.11	0.88	186.5
0.1	1340	129.9	6479	25.6	439	5.912	0.7853	6.31	15.6
0.14	1319	135.0	6962	27.8	449	4.790	0.62	6.7	13.05
0.16	1279	145.0	7952	31.9	466	3.093	0.39	7.51	9.43
0.2	1289	143.4	7704	30.8	459	3.414	0.4341	7.34	10.63
0.25	1268	146.3	8235	33.	474	2.809	0.3454	7.72	8.51
0.3	1262	149.3	8396	33.4	474	2.702	0.3319	7.86	8.42
0.4	1261	149.5	8424	33.5	474	2.687	0.3305	7.9	8.59
0.5	1249	150.5	8758	33.2	474	2.585	0.3170	8.21	8.42
0.6	1240	151.5	9014	33.1	475	2.488	0.3055	8.44	8.51
0.7	1233	152.8	9214	33.2	476	2.361	0.2893	8.62	8.22
0.8	1232	153.	9242	33.2	476	2.345	0.2869	8.64	8.17
0.9	1232	153.	9242	33.3	476	2.345	0.2869	8.64	8.17
0.99	1200	160.	10212	36.6	472	1.795	0.2215	9.59	7.02
					STS-3				
0.025	1630	39.1	772	5.1	384	423.2	64.33	0.8	182.7
0.1	1252	131.4	6386	26.6	447	6.032	0.7973	6.17	16.32
0.14	1183	149.2	8100	32.7	480	2.959	0.3591	7.54	8.31
0.16	1183	149.2	8100	32.7	480	2.959	0.3591	7.54	8.91
0.2	1183	149.2	8100	32.7	480	2.959	0.3591	7.54	8.91
0.25	1183	149.2	8100	32.7	480	2.959	0.3591	7.54	8.41
0.3	1183	149.2	8100	32.7	480	2.959	0.3591	7.54	8.91
0.4	1183	149.2	8100	32.7	480	2.959	0.3591	7.54	8.91
0.5	1183	149.2	8100	32.7	480	2.959	0.3591	7.54	8.93
0.6	1148	153.9	9084	33.5	482	2.473	0.2990	8.44	8.25
0.7	1120	159.4	9911	36.0	482	2.006	0.2424	9.21	7.34
0.8	1107	162.6	10329	37.5	480	1.772	0.2152	9.62	6.41
0.9	1106	162.9	10362	37.5	480	1.755	0.2132	9.65	6.77
0.99	1182	168.7	11134	38.7	474	1.402	0.1723	10.43	5.34
					STS-4				
0.025	1524	43.8	880	5.6	382	345.2	52.7	0.92	171.2
0.1	1178	129.	6510	24.9	454	7.309	0.9381	6.23	19.56
0.14	1152	135.8	7201	27.1	461	5.538	0.6994	6.84	15.93
0.16	1131	142.7	7805	29.2	472	4.221	0.5207	7.33	12.61
0.2	1028	174.7	11028	40.4	478	1.218	0.1486	10.3	5.04
0.25	1028	174.7	11028	40.4	478	1.218	0.1486	10.3	5.34
0.3	1028	174.7	11028	40.4	478	1.218	0.1486	10.3	5.04
0.4	1028	174.7	11028	40.4	478	1.218	0.1486	10.3	5.04
0.5	1028	174.7	11028	40.4	478	1.218	0.1486	10.3	5.04
0.6	1028	174.7	11028	40.4	478	1.218	0.1486	10.3	5.04
0.7	1027	175.2	11058	40.4	477	1.194	0.1459	10.33	4.97
0.8	1029	174.1	10998	40.3	479	1.242	0.15.4	10.26	5.18
0.9	1028	174.7	11028	40.4	478	1.218	0.1486	10.3	5.04
0.99	1029	174.1	10998	40.3	479	1.242	0.1514	10.26	5.22
					STS-5				
0.025	1607	41.3	839	6.9	391	373.9	55.82	0.87	169.7
0.1	1215	135.8	6893	27.9	442	5.224	0.6895	6.69	15.57
0.14	1140	154.7	8881	35.1	457	2.418	0.3085	8.48	8.73
0.16	1140	154.5	8881	35.1	457	2.418	0.3085	8.48	8.73
0.2	1140	154.5	8881	35.1	457	2.418	0.3085	8.48	8.73
0.25	1125	157.9	9328	36.7	458	2.108	0.2684	8.90	7.97
0.3	1125	157.9	9328	36.7	458	2.108	0.2684	8.90	7.97
0.4	1125	157.9	9328	36.7	458	2.108	0.2684	8.90	7.97
0.5	1125	157.9	9328	36.7	458	2.108	0.2684	8.90	7.97
0.6	1122	158.5	9406	37.0	457	2.057	0.2625	8.98	7.87
0.7	1122	158.5	9406	37.0	457	2.057	0.2625	8.98	7.87
0.8	1122	158.5	9406	37.0	457	2.057	0.2625	8.98	7.87
0.9	1118	159.8	9563	37.5	455	1.955	0.2506	9.15	7.67
0.99	1120	159.1	9484	37.3	456	2.006	0.2565	9.06	7.77

[a]Instruments at x = 0.29L and 0.95L have been omitted because of redundancy and data quality.

TABLE IV.- LOCAL FLOW CONDITIONS AT TIMES OF BOUNDARY LAYER TRANSITION ALONG THE ORBITER WINDWARD PITCH PLANE

$\frac{x_{tr}^a}{L}$	Time, sec	M	$Re_x \times 10^{-6}$	$\frac{Re_\theta}{M}$	T_w, °R	$\frac{T_w}{T_o}$	Re_k, k (in.) = 0.03	0.06	0.1
STS-1									
0.025	1716	0.67	4.93	991	849	1.94	4145	9019	15100
0.1	1357	1.96	1.96	247	1264	0.478	155	494	1129
0.2	1272	2.03	1.56	218	1869	0.447	63	189	404
0.26	1231	1.84	1.37	208	1403	0.287	49	142	292
0.4	1139	2.01	1.73	217	1615	0.263	39	108	214
0.5	1136	2.01	2.14	240	1597	0.258	37	104	206
0.6	<1052	2.20	2.27	239	1517	0.183	31	82	163
0.7									
0.8	No data prior to 1052 sec.								
0.9									
0.99									
STS-2									
0.025	1710	0.8	4.45	819	630	1.44	3572	8112	13650
0.1	1340	2.06	1.26	205	1540	0.443	111	336	734
0.2	1289	2.05	1.48	211	1421	0.322	62	182	387
0.26	1268	1.94	1.63	217	1410	0.296	59	163	339
0.4	1261	2.05	2.69	274	1414	0.289	53	158	331
0.5	1249	2.11	3.37	300	1421	0.28	52	153	321
0.6	1240	2.15	3.91	321	1346	0.257	49	147	307
0.7	1233	2.15	4.44	338	1321	0.248	46	138	289
0.8	1232	2.15	5.04	362	1346	0.252	45	134	282
0.9	1232	2.31	4.95	342	1309	0.245	34	104	222
0.99	1200	2.29	3.7	293	1086	0.189	24	73	154
STS-3									
0.025	1630	0.74	4.35	881	850	1.96	3468	7909	13320
0.1	1252	2.0	1.24	208	1400	0.411	117	337	733
0.2	1183	1.89	1.19	199	1460	0.313	55	159	331
0.26	1183	1.92	1.6	221	1390	0.298	57	167	348
0.4	1183	2.04	2.84	269	1434	0.306	56	167	353
0.5	1183	2.04	3.55	316	1379	0.294	53	153	337
0.6	1148	2.10	3.84	319	1355	0.257	50	147	307
0.7	1120	2.02	2.81	321	1472	0.262	45	131	268
0.8	1107	1.99	4.04	334	1414	0.245	42	121	247
0.9	1106	2.13	3.81	310	1397	0.241	31	93	192
0.99	1082	2.24	3.26	278	1036	0.170	23	67	138
STS-4									
0.025	1524	0.83	4.1	748	866	1.94	3222	7445	12560
0.1	1178	2.10	1.52	221	1501	0.427	137	413	902
0.2	1028	1.57	0.6	155	1826	0.311	32	86	168
0.26	1028	1.62	0.81	169	1635	0.277	35	92	179
0.4	1028	1.82	1.49	213	1746	0.293	36	98	193
0.5	1028	1.82	1.86	237	1578	0.265	35	99	188
0.6	1028	1.82	2.29	259	1511	0.253	34	94	186
0.7	1027	1.82	2.56	277	1472	0.246	32	91	181
0.8	1029	1.82	3.01	303	1570	0.247	32	92	185
0.9	1028	1.97	2.9	282	1460	0.245	25	73	149
0.99	1029	2.08	2.85	271	1406	0.236	21	61	126
STS-5									
0.025	1607	0.78	3.74	776	822	1.96	3216	7319	12320
0.1	1215	1.94	1.13	201	1471	0.387	108	317	674
0.2	1140	1.81	1.02	194	1578	0.311	53	151	304
0.26	1125	1.76	1.22	203	1530	0.290	52	144	287
0.4	1125	1.92	2.23	256	1482	0.278	52	148	302
0.5	1125	1.92	2.76	285	1481	0.278	50	144	295
0.6	1122	1.90	3.24	311	1395	0.260	47	138	284
0.7	1122	1.90	3.77	335	1321	0.247	46	135	279
0.8	1122	1.90	4.34	360	1395	0.260	45	133	275
0.9	1118	2.02	4.04	334	1347	0.249	34	102	213
0.99	1120	2.15	4.07	322	1134	0.211	27	83	177

[a]Locations limited to DFI stations where local flow correlations were developed.
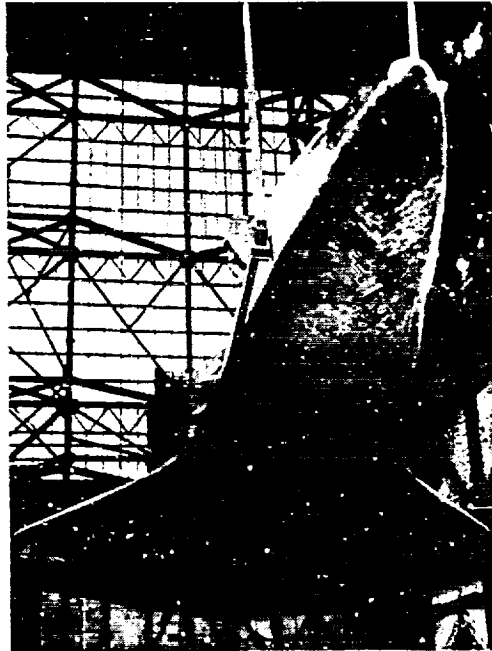
Figure 1.- Photograph of Columbia (OV-102) windward surface showing the
TPS tiles and resulting distributed roughness caused by tile
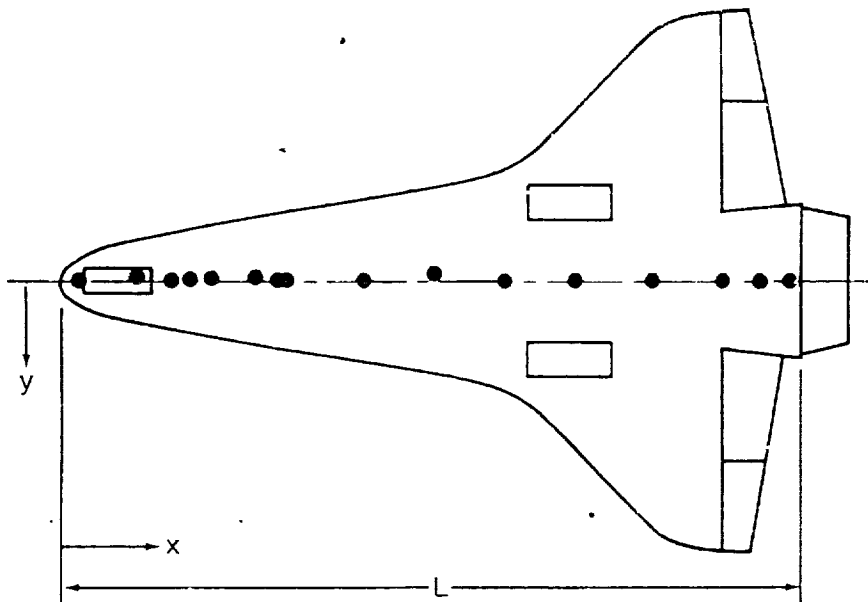gaps and misalignments.

Figure 2.- Locations of surface temperature measurements along orbiter windward
centerline. See Table I for detailed locations and instrument numbers.
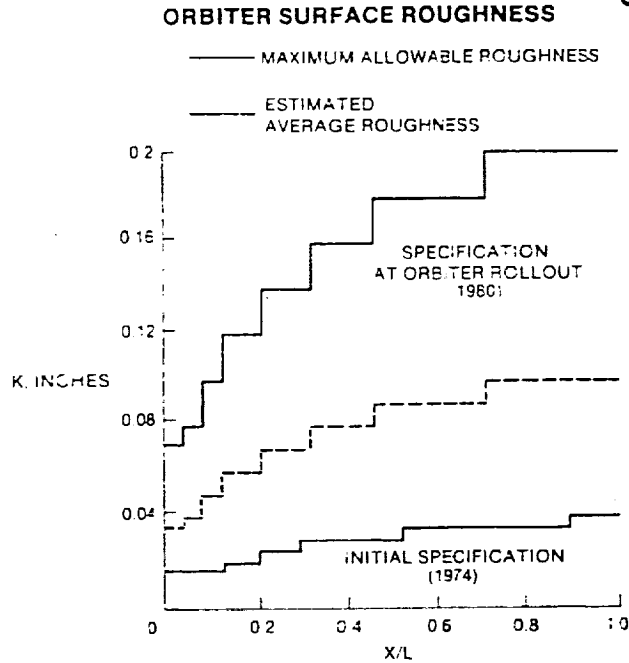
ORBITER SURFACE ROUGHNESS

———— MAXIMUM ALLOWABLE ROUGHNESS

——— ESTIMATED
AVERAGE ROUGHNESS

Figure 3.- Distribution of maximum allowable and estimated average surface roughness for the orbiter centerline.

**COMPARISON OF
ORBITER FREE-STREAM
FLOW CONDITIONS**
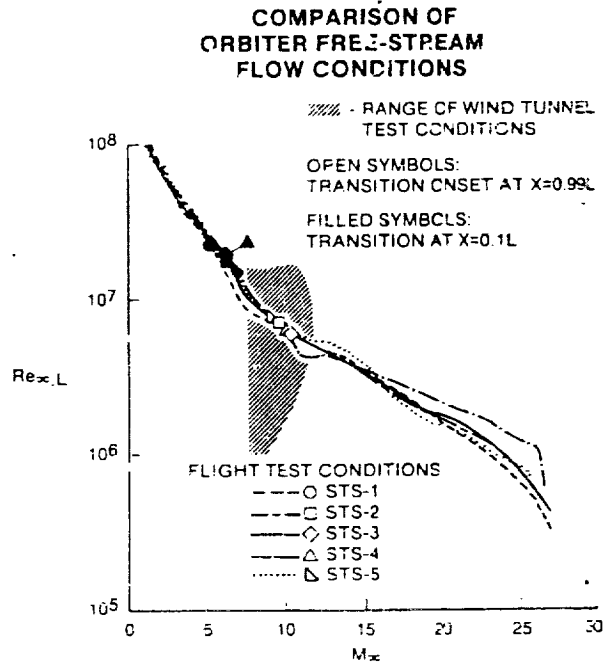
Figure 4.- Comparison of free-stream flow parameters for flight and wind tunnel test conditions.

FREE-STREAM REYNOLDS NUMBER HISTORIES

OPEN SYMBOLS:
TRANSITION ONSET X=0.99L

FILLED SYMBOLS:
TRANSITION AT X=0.1L

$Re_{\infty,L}$

RANGE OF $Re_{\infty,L}$
FOR WIND TUNNELS

———O STS-1
———◻ STS-2
———◇ STS-3
——·—△ STS-4
········◻ STS-5

ENTRY TIME (SEC)
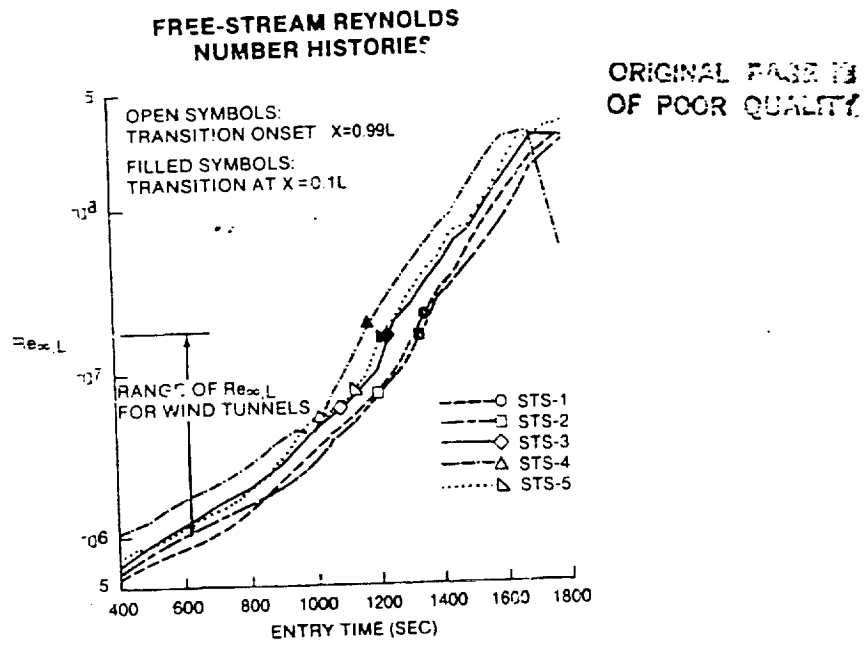
Figure 5.- Histories of free-stream Reynolds numbers for the STS trajectories.

ANGLE OF ATTACK HISTORIES

OPEN SYMBOLS:
TRANSITION ONSET: X = 0.99L

FILLED SYMBOLS:
TRANSITION AT X = 0.1L

O ——— STS-1
◻ ——— STS-2
◇ ——— STS-3
△ —·—STS-4
◻ ········STS-5

ANGLE
OF
ATTACK
DEGREES

ENTRY TIME (SEC)
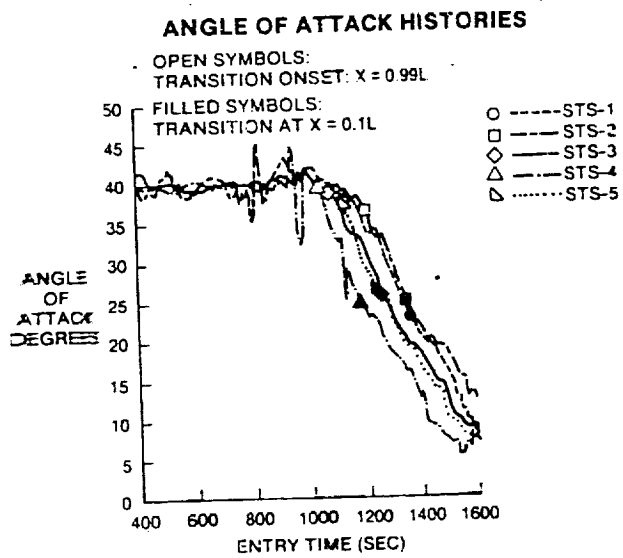
Figure 6.- Angle of attack histories for the STS trajectories.

77
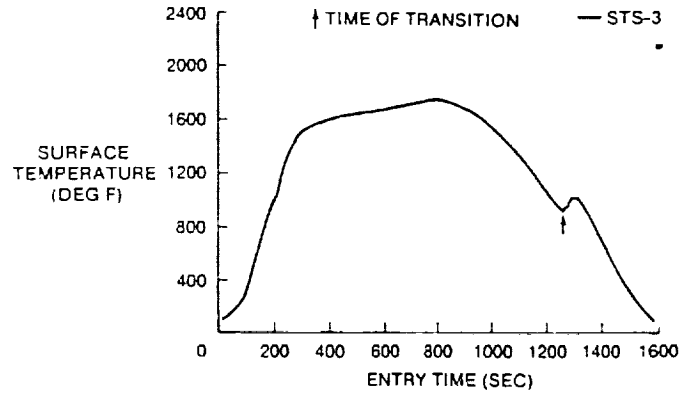
(a) x = 0.1L.
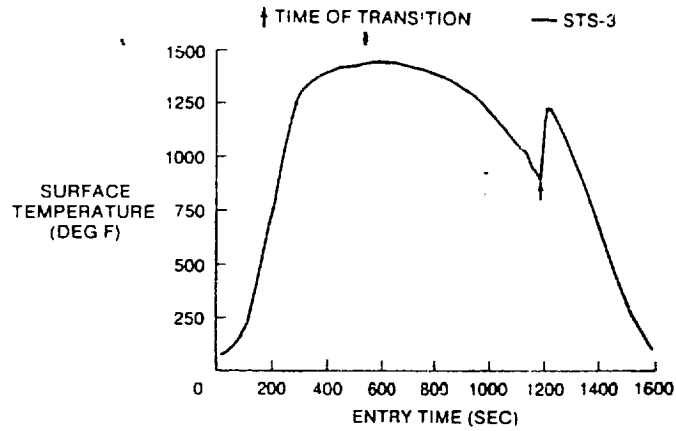
(b) x = 0.5L.

Figure 7.- Typical surface temperature histories used to locate times of transition.

TIME OF TRANSITION — STS-3
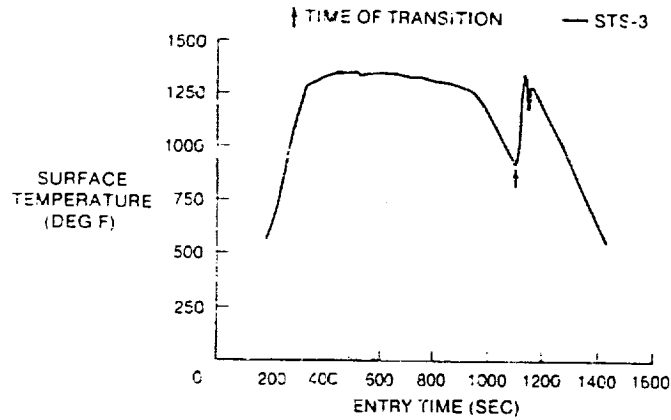
(c) x = 0.9L.

Figure 7.- Concluded.

**COMPARISON OF FREE-STREAM
FLOW CONDITIONS
FOR ORBITER TRANSITION**

---- DATA FAIRING (SMOOTH MODEL)
--- DATA FAIRING (ROUGH MODEL) AEDC-F
—— DATA FAIRING (ROUGH MODEL) AEDC-B
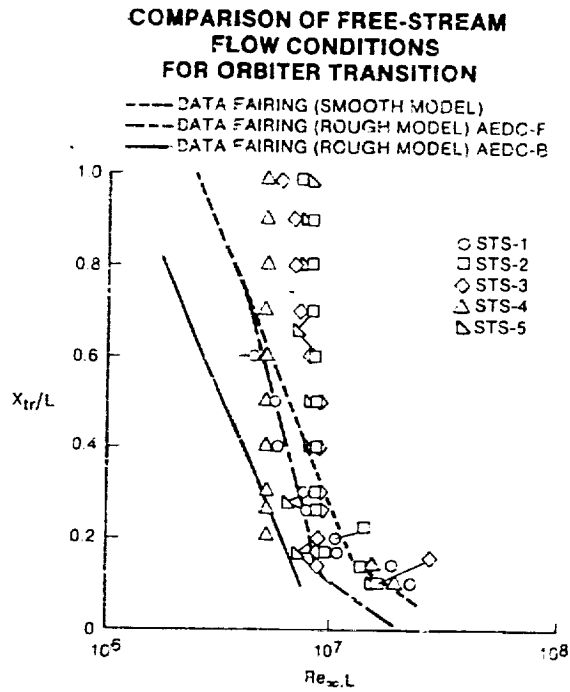
Figure 7.- Comparisons of $Re_{\infty,L}$ for transition along the orbiter windward pitch plane at flight and wind tunnel conditions.
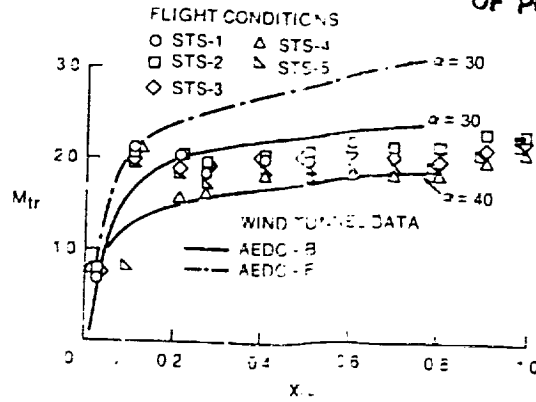
(a) Mach number.
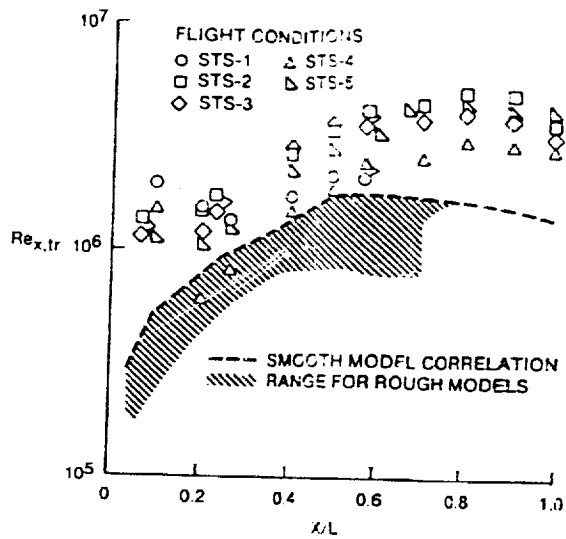
(b) $Re_{x,tr}$.

Figure 9.- Comparisons of local flow conditions for transition along the orbiter windward pitch plane at flight and wind tunnel conditions.
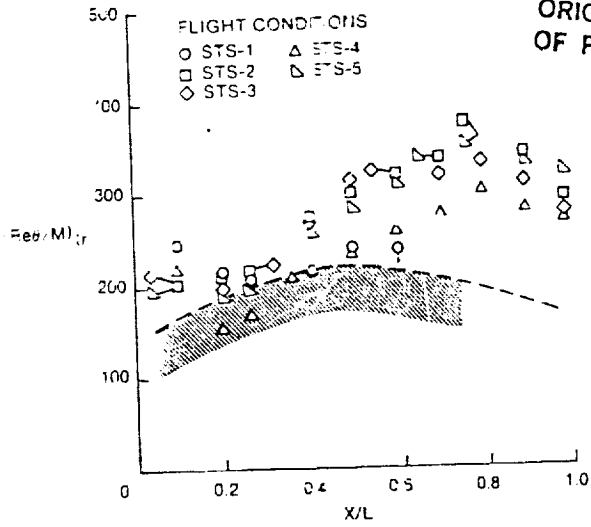
(c) $(Re\theta/M)_{tr}$.
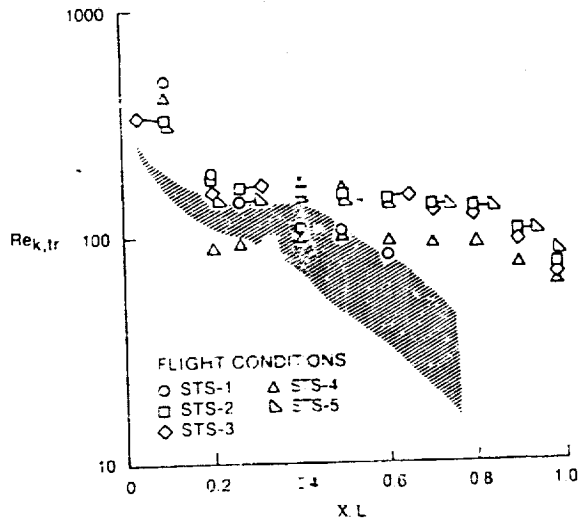
(d) $Re_{k,tr}$.

Figure 9.- Concluded.

**TRANSITION CORRELATION
FROM WIND TUNNEL DATA**
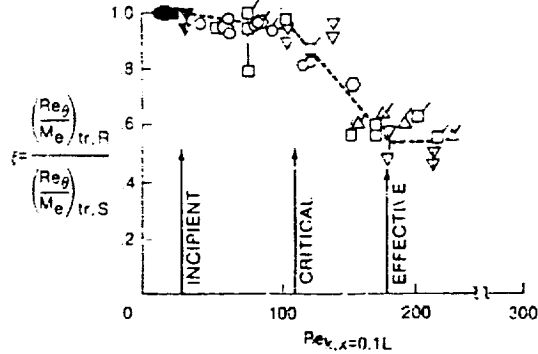
Figure 10.— Correlation of the relative transition parameter as a function of $Re_{k,x=0.1L}$ (Ref. 7).
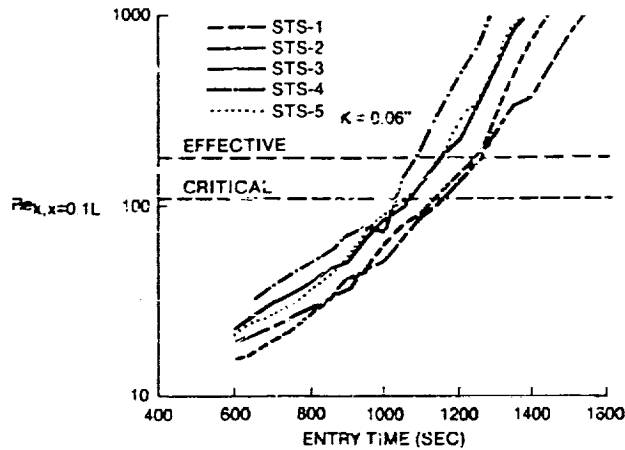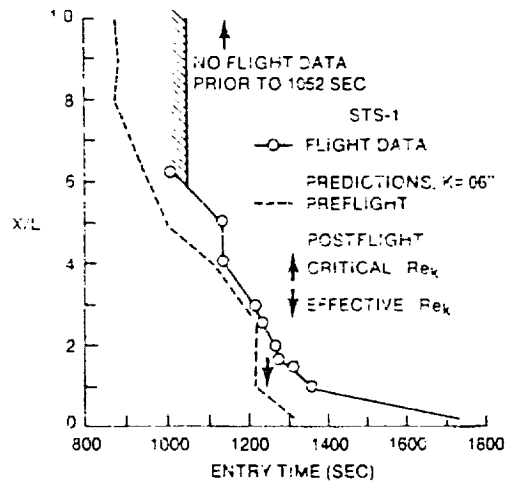
**HISTORIES OF REFERENCE
ROUGHNESS REYNOLDS NUMBERS**

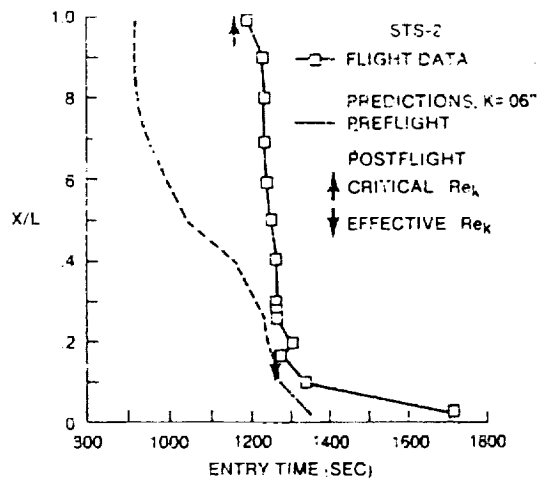Figure 11.— Histories of $Re_{k,x=0.1L}$ for $k = 0.06"$ for the STS trajectories.

776

**COMPARISONS OF PREDICTED
AND MEASURED TRANSITION TIMES**
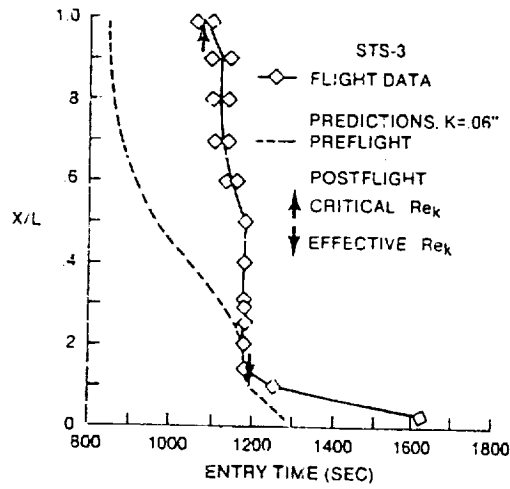
(a) STS-1.

**COMPARISONS OF PREDICTED
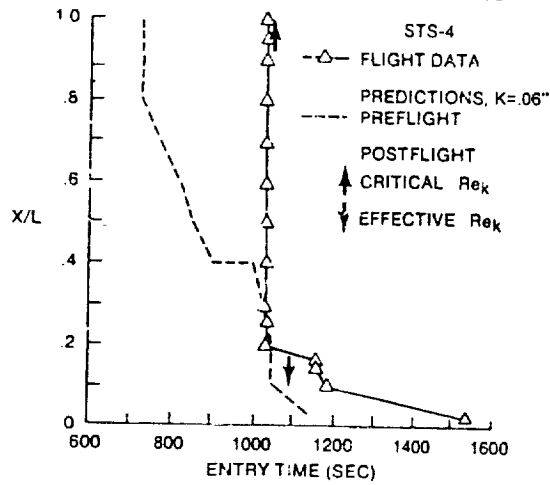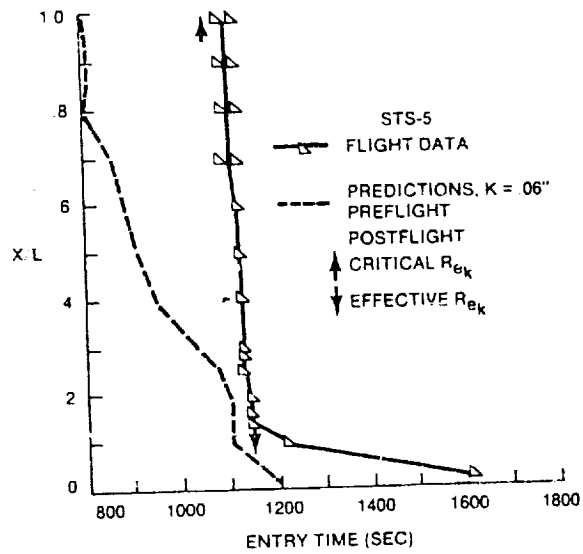AND MEASURED TRANSITION TIMES**

(b) STS-2.

Figure 12.- Comparisons of predicted and measured transition times for the first five STS trajectories.

**COMPARISONS OF PREDICTED
AND MEASURED TRANSITION TIMES**

STS-3
◇— FLIGHT DATA

PREDICTIONS, K=.06"
- - - PREFLIGHT

POSTFLIGHT
↑ CRITICAL Re_k
↓ EFFECTIVE Re_k

X/L

ENTRY TIME (SEC)

(c) STS-3.

**COMPARISONS OF PREDICTED
AND MEASURED TRANSITION TIMES**

STS-4
△— FLIGHT DATA

PREDICTIONS, K=.06"
- - - PREFLIGHT

POSTFLIGHT
↑ CRITICAL Re_k
↓ EFFECTIVE Re_k

X/L

ENTRY TIME (SEC)

(d) STS-4.

Figure 12.- Continued.

**COMPARISONS OF PREDICTED
AND MEASURED TRANSITION TIMES**

STS-5

FLIGHT DATA

PREDICTIONS, K = .06"
PREFLIGHT
POSTFLIGHT
CRITICAL R_{e_k}
EFFECTIVE R_{e_k}

X/L

ENTRY TIME (SEC)

(e) STS-5.

Figure 12.- Concluded.